Inversion of Shear Wave Anisotropic Parameters in Strongly Anisotropic Formations

Shihong Chi[1], Xiaoming Tang[2], and Zhenya Zhu[1]

[1]Earth Resources Laboratory
Dept. of Earth, Atmospheric and Planetary Sciences
Massachusetts Institute of Technology
Cambridge, MA 02142

[2]Baker Atlas
2001 Rankin Road,
Houston, TX 77073

ABSTRACT

Deepwater reservoirs use highly deviated wells to reduce cost and enhance hydrocarbon recovery. Due to the strong anisotropic nature of many of the marine sediments, anisotropic seismic imaging and interpretation can improve reservoir characterization. Sonic logs acquired in these wells are strongly dependent on well deviations. Cross-dipole sonic logging provides apparent shear wave anisotropy in deviated wells, which can be far from the truth. Although anisotropic parameters have been successfully obtained using data from wells of several deviations or using single well data based on weak anisotropy approximation, estimation of strong shear wave anisotropy from single well data remains a challenge.

Using sensitivity analysis, we find Stoneley wave velocity has good sensitivity to qSV and SH wave velocities in deviated wells. We create a linear inversion scheme to estimate shear wave anisotropy using SH, SV, and Stoneley wave velocities logged in one well. We first apply the method to laboratory measurements from boreholes of various deviations relative to the symmetry axis of an anisotropic material. We then apply the method to a field data set acquired in a deviated well. We also compute the vertical and horizontal shear wave velocity logs in this well using the inverted elastic shear wave constants.

INTRODUCTION

In recent years, significant discoveries of hydrocarbon reservoirs have been made in the deepwater fields. Offshore development uses high-angle wells to reduce drilling cost and enhance recovery. Since these offshore reservoir formations often exhibit strong anisotropy, it becomes very important to take into account anisotropy in sonic and seismic data processing and interpretation (Tsvankin, 1995, Ren et al., 2005). For example, converted P-S waves can image through a gas cloud that would obstruct P wave imaging because shear waves are sensitive to theformation frame but not the fluid content. Therefore, when we can obtain both P and S wave images, they show different amplitude and polarization. Joint interpretation of the data may yield formation fluid

information that cannot be obtained by P wave data alone (Zhu et al., 1999, Li et al., 2001). Anisotropy information is crucial for such application as well as for standard P wave imaging.

Sonic logging data provide high-resolution formation velocity measurements for seismic imaging and other interpretation techniques. However, the velocities acquired in deviated wells penetrating anisotropic formations can be significantly different from the vertical velocities (Furre and Brevik, 1998). Therefore, inversion of anisotropic parameters and correction to sonic logs obtained in deviated wells are necessary.

Tang (2003) developed an inversion method to determine shear wave anisotropy using shear and Stoneley wave data measured in vertical wells. For deviated wells, people routinely use cross-dipole sonic logging data to estimate formation shear wave anisotropy of a transversely isotropic formation with vertical rotational symmetric axis (TIV formation). The SH and SV velocities measured by cross-dipole tools vary with well deviations and are not the horizontal and vertical shear wave velocities except in horizontal wells. Therefore, the anisotropy obtained using cross-dipole data is an apparent anisotropy and may not be the true formation shear wave anisotropy. Zhu et al. (2006) showed shear wave velocity variations with well deviations for a Phenolite model (Figure 1a). Figure 1b shows apparent cross-dipole anisotropy varies with well deviation significantly and does not measure the true formation shear wave anisotropy except in a horizontal well. Tang and Patterson (2005) provided field examples of anisotropy variation with well deviations. One of their examples shows that shear wave anisotropy goes through a 90 degree azimuth change through a transition angle. Below this angle, the fast shear is the qSV wave. Above this angle, the fast shear becomes the SH wave, as explained by the theoretical curves in Figure 1.

Norris and Sinha (1993) showed how to determine the parameters for weak anisotropy in deviated wells using data from one well, but their method may not work well for strongly anisotropic formations. The previously described methods limit their applications to vertical wells or deviated wells in weak anisotropic formations.
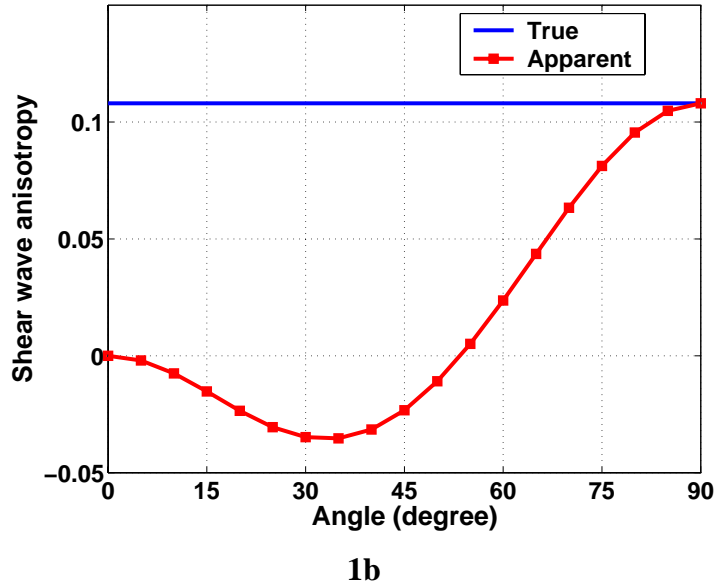

1a

1b
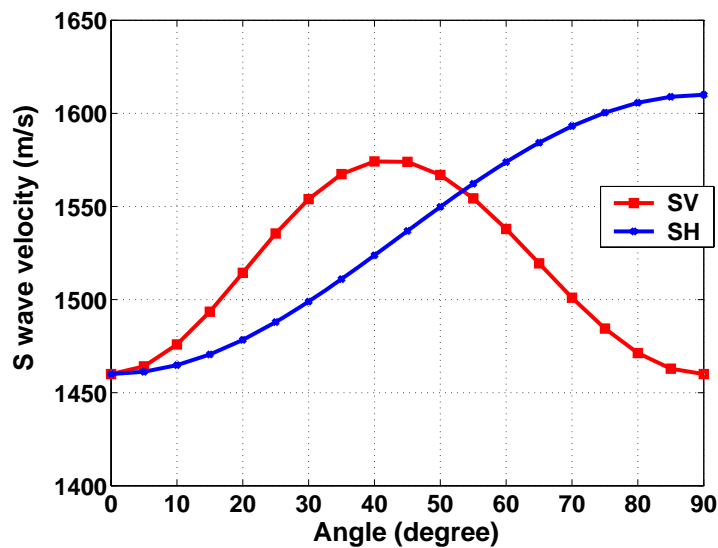
Figure 1: Shear wave (SH and SV) velocities and apparent anisotropy at various well deviations

Hornby et al. (2003) created an iterative inversion scheme to invert shale anisotropy parameters using multiple wells penetrating shale sections at different angles. The inversion involves fitting the sonic log data at a range of borehole angles to the compressional group velocity surface. Thomsen anisotropic parameters, ε and δ, and vertical P wave velocity are obtained. These information are very important for P wave seismic imaging and reservoir analysis. For converted PS wave imaging and anisotropy analysis for reservoir properties using shear wave data, inversion of shear wave anisotropic parameter is necessary.

We attempt to develop a method that can extract anisotropy parameters, particularly the shear wave anisotropic parameter, in strongly anisotropic formations. We apply our method to our laboratory data and a set of field data. We also address the issue of using log data acquired in dipping formations using the field example.

BASIC THEORY

A TI formation is described by the following 6x6 elastic stiffness matrix, in which five elastic constants are independent:

$$C = \begin{bmatrix} c_{11} & c_{12} & c_{13} & & & \\ & c_{11} & c_{13} & & & \\ & & c_{33} & & & \\ & & & c_{44} & & \\ & & & & c_{44} & \\ & & & & & c_{66} \end{bmatrix}$$

(1)

In the above matrix, the elements are zero in upper matrix except those filled in. The matrix is symmetric. It is also should be noted that $c_{12} = c_{11} - 2c_{66}$.

In TI media, the qP and qSV wave phase velocities are dependent on their propagation direction. Daley and Hron (1977) gave the following formulae:

$$\rho V_{qP}^2(\theta) = \frac{1}{2}\left[c_{33} + c_{44} + (c_{11} - c_{33})\sin^2\theta + D(\theta) \right],$$

$$\rho V_{qSV}^2(\theta) = \frac{1}{2}\left[c_{33} + c_{44} + (c_{11} - c_{33})\sin^2\theta - D(\theta) \right],$$

(2)

where ρ is density of the media and phase angle θ is the angle between the wavefront normal and the rotational symmetry axis. $D(\theta)$ is a compact notation for the quadratic combination:

$$D(\theta) \equiv \left\{ (c_{33} - c_{44})^2 + 2\left[2(c_{13} + c_{44})^2 - (c_{33} - c_{44})(c_{11} + c_{33} - 2c_{44}) \right]\sin^2\theta \right.$$
$$\left. + \left[(c_{11} + c_{33} - 2c_{44})^2 - 4(c_{13} + c_{44})^2 \right]\sin^4\theta \right\}^{1/2}$$

(3)

and

$$\rho V_{SH}^2 = c_{44}\cos^2\theta + c_{66}\sin^2\theta .$$

(4)

From equations (2), (3), and (4), we obtain equations for calculating the vertical and horizontal formation moduli for P and S wave propagation as:

$$c_{44} = \rho V_{SV}^2,$$

(5)

$$c_{66} = \rho V_{SH}^2,$$

(6)

$$c_{33} = \rho V_{PV}^2,$$

(7)

$$c_{11} = \rho V_{PH}^2,$$

(8)

and

$$c_{12} = c_{11} - 2c_{66}.$$

(9)

where ρ is the bulk density, V_{PH} and V_{SH} are the horizontal P and S wave velocities, and V_{PV} and V_{SV} are the vertical P and S wave velocities. Using P or S wave phase velocities at 45 degrees, we express c_{13} as (Hornby et al., 2003)

$$c_{13} = -c_{44} \pm \left[(c_{11} + c_{44} - 2\rho V_{45}^2)(c_{33} + c_{44} - 2\rho V_{45}^2) \right]^{1/2}$$

(10)

where V_{45} is a compressional (qP) or shear (qSV) wave velocity taken at angle of 45 degrees relative to the axis of symmetry, and the minus sign and the plus sign are for qP and qSV wave velocity, respectively. Thomsen (1986) defined three anisotropic parameters, $\varepsilon, \delta, \gamma$, as follows:

$$\varepsilon = \frac{c_{11} - c_{33}}{2c_{33}}, \tag{11}$$

$$\delta = \frac{\left(c_{13} + c_{44}\right)^2 - \left(c_{33} - c_{44}\right)^2}{2c_{33}\left(c_{33} - c_{44}\right)}, \tag{12}$$

$$\gamma = \frac{c_{66} - c_{44}}{2c_{44}}, \tag{13}$$

for characterizing anisotropy of TIV media.

ESTIMATION OF SHEAR WAVE ANISOTROPY USING SONIC LOGGING DATA IN A DEVIATED WELL

We first investigate how to use acoustic logging in deviated including horizontal wells to resolve the two shear moduli c_{44} and c_{66}, which determine the shear-wave propagation characteristics in a TI formation. From inverted shear moduli c_{44} and c_{66}, the shear-wave TI parameter γ can be simply calculated. We also explore means to obtain the shear-wave TI parameter using cross-dipole and Stoneley-wave measured anisotropy in deviated wells.

Sensitivity analysis

To study the feasibility of using cross-dipole and Stoneley-wave data to determine anisotropic information in deviated wells, we conduct a sensitivity analysis using the theory of partition coefficients (equivalent to normalized partial derivatives, see Cheng et al., 1982, Ellefsen et al., 1992). We use the VTI formation properties described in Zhu et al. (2006) in our analysis (Table I). The fluid density is 1000 kg/m^3.

In a deviated well penetrating a TIV formation, horizontally polarized SH wave velocity is sensitive to horizontal and vertical shear wave velocities according to equation (4). Furthermore, Figure 3a shows that in a vertical well, the SH wave velocity is only sensitive to the vertical shear wave velocity; but as well deviation increases, the SH wave velocity becomes more sensitive to the horizontal shear wave velocity. The qSV wave polarizes normal to the borehole axis and its velocity is sensitive to formation properties along the borehole axis direction Figure 3b shows that the qSV wave velocity is controlled by the vertical shear wave velocity in near vertical or horizontal wells. However, it is not sensitive to the shear wave velocity around 45 degree well deviation. It is sensitive to the P wave velocities instead.

At low frequencies, the Stoneley wave radially deforms the borehole, and the Stoneley wave velocity provides an independent measurement of formation properties transverse

to the borehole axis. Integration of SH, qSV and Stoneley velocity measurements may provide sufficient information to invert shear wave anisotropy using single well data.

Chi and Tang (2006) derived a three-dimensional analytical solution for low frequency Stoneley-wave velocity in deviated boreholes penetrating a transversely isotropic with a vertical symmetry axis (VTI) or general anisotropic formation. The sensitivity of the Stoneley-wave velocity in a slow TIV formation can be partitioned into six model parameters: the borehole fluid velocity V_f, formation horizontal shear velocity $V_{sh} = \sqrt{c_{66}/\rho}$, vertical shear velocity $V_{sv} = \sqrt{c_{44}/\rho}$, horizontal compressional velocity $V_{ph} = \sqrt{c_{11}/\rho}$, vertical compressional velocity $V_{pv} = \sqrt{c_{33}/\rho}$ and the modulus c_{13}. The sensitivity is defined as the normalized partial derivatives $[V_\gamma/V_{ST}(\theta)][\partial V_{ST}(\theta)/\partial V_\gamma]$, where the subscript γ denotes the subscripts *f, sv, sh, ph, pv*, and c_{13}, respectively. The Stoneley-wave phase velocity $V_{ST}(\theta)$ is calculated using the 3-D analytical solution in the absence of a logging tool.

As Figure 3c shows, Stoneley-wave sensitivity to the VTI formation is mostly controlled by V_{sh} or c_{66} in a vertical well. The sensitivity decreases as the well deviation increases. With increasing well deviation, V_{sv} or c_{44} becomes an important parameter to affect the Stoneley-wave propagation velocity. It can be seen that the summation of the three sensitivities of V_f, V_{sv} or c_{44} and V_{sh} or c_{66}, is close to 1 at small deviation. According to the theory of partition coefficients, this indicates that the Stoneley wave sensitivity to other TI parameters, $c_{11}, c_{13},$ and c_{33}, is low at relatively small deviation for this slow TI formation. From the sensitivity analysis of Stoneley-wave velocity to various model parameters, we can see that for a well deviation up to 30°, the velocity is mainly controlled by V_{sh} or c_{66}. Within this deviation range, the sensitivity to V_{sh} or c_{66} is more than twice that of V_{sv} or c_{44}. Thus, the method for determining formation shear wave transverse isotropy developed for a vertical well (Tang, 2003) can still be applied in a moderately deviated well. For wells with higher deviation, Stoneley wave velocity sensitivity to V_{sv} or c_{44} increases and becomes higher than it to V_{sh} or c_{66} at round 50 degrees (Figure 3c). Horizontal V_{sh} or c_{66} cannot be estimated robustly from the Stoneley wave velocity in highly deviated wells. The qSV velocity also becomes much higher than the vertical shear wave velocity. Therefore, the method that works well for a vertical well cannot accurately determine shear wave anisotropy for a highly deviated well. We may have to integrate Stoneley data with other acoustic logging measurements such as qSV and SH wave velocities to determine the shear wave anisotropy.
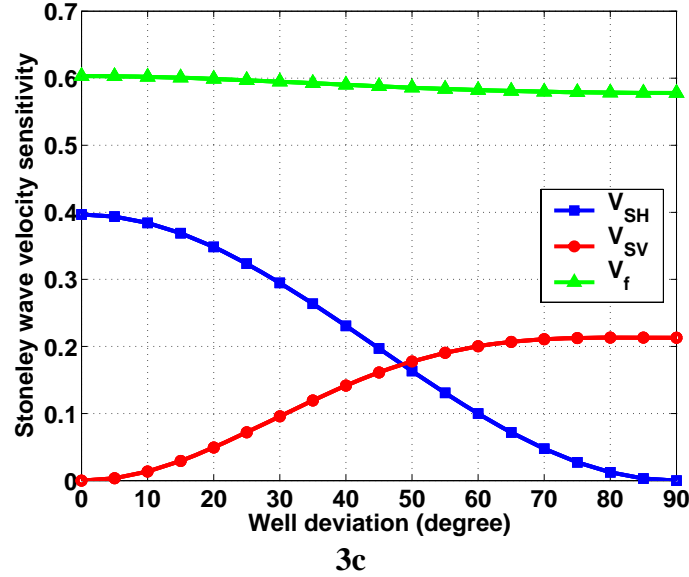
3a

3b

3c
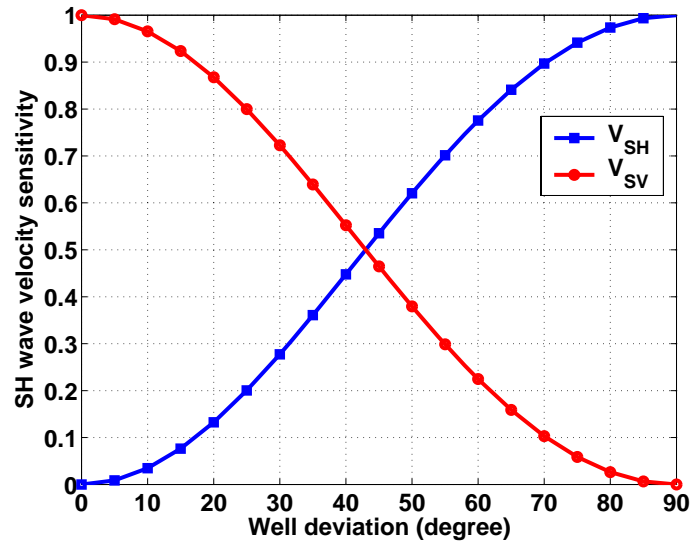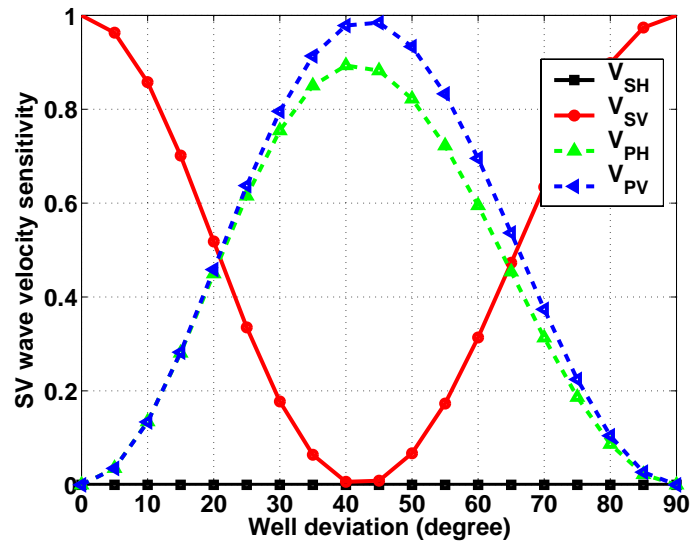
Figure 3: (a) SH and (b) SV wave velocity sensitivities to the formation shear wave velocities. (c) Stoneley wave sensitivity to fluid compressional velocity and formation shear wave velocities.

Approximations for qP, qSV, and Stoneley velocities

Because the analytical formulation for qP, qSV, and Stoneley wave velocities are nonlinear and complicated in terms of the elastic stiffnesses, we seek a good approximation that can lead to a linear inversion of the shear moduli and shear anisotropic parameter.

Although Norris and Sinha (1995) obtained relatively simple expressions for qSV and Stoneley wave velocities using the first order perturbation method, Chi and Tang (2003) derived better approximations of the moduli of qP, qSV, and Stoneley waves in cases of any well deviation and strong anisotropy. Figure 4 shows that Chi and Tang's approximations are better than those obtained by weak anisotropy approximation for a Phenolite model (Zhu et al., 2006). For qP wave velocity (Figure 4a), Thomsen's approximation works well only for small phase angles; the weak anisotropy approximation is fairly accurate; and Chi and Tang's approximation almost overlays with the theory. Figure 4b shows that for the qSV wave velocity, Thomsen's and the weak anisotropy approximations work almost equally well at all phase angles, but at around 45 degrees, Chi and Tang's approximation works much better. For Stoneley wave velocity, Figure 4c shows that Rice's model introduces the biggest error (Rice, 1987), and Chi and Tang's approximation still performs the best. The approximations have common terms involving elastic stiffnesses, but the constant coefficients of these terms are different. Combining the formula of the modulus of SH waves, we can solve for the shear moduli c_{44} and c_{66}.

In deviated wells, the *qSV* and Stoneley wave moduli are approximated as follows:

$$\mu_{qP} = \rho V_{qP}^2 = c_{11} \sin^2 \theta + c_{33} \cos^2 \theta - \frac{2(\varepsilon - \delta) c_{33} \sin^2 \theta \cos^2 \theta}{1 + 2\varepsilon \sin^2 \theta / f} \ . \tag{14}$$
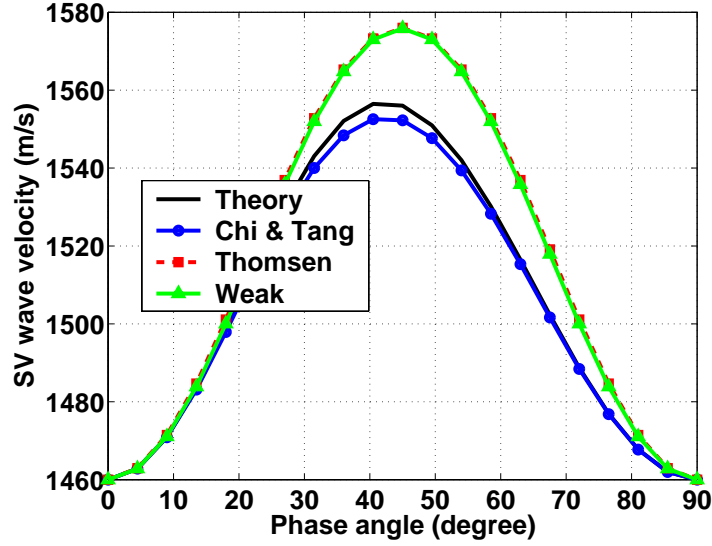
$$\mu_{qSV} = \rho V_{qSV}^2 = c_{44} + \frac{2(\varepsilon - \delta) c_{33} \sin^2 \theta \cos^2 \theta}{1 + 2\varepsilon \sin^2 \theta / f} \ , \tag{15}$$

$$\mu_{ST} = c_{44} \sin^2 \theta + c_{66} \cos^2 \theta + \frac{1}{4} \frac{(\varepsilon - \delta) c_{33} \sin^4 \theta}{1 + 2\varepsilon \sin^2 \theta / f} \ , \tag{16}$$
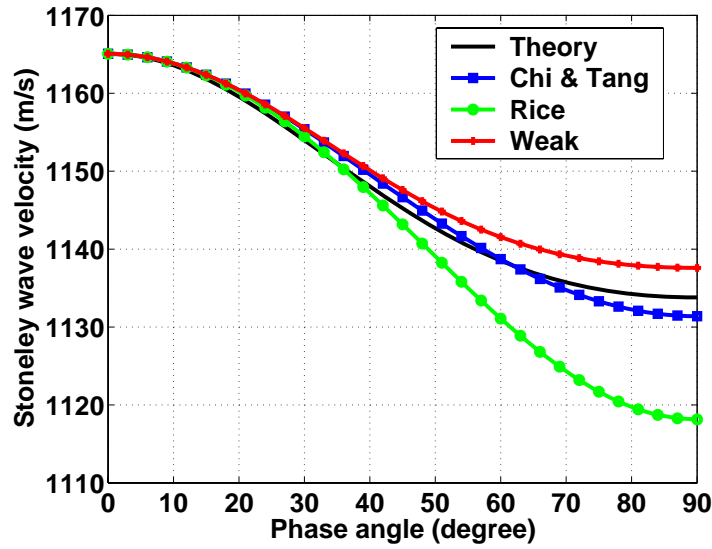
where $f = 1 - \dfrac{c_{44}}{c_{33}}$. These approximations are compared with other existing ones in modeling the velocity of qSV, and qP waves in various formations. From Figures 4a and 4b, we can see the new approximations are far more accurate for large anisotropy and large well deviations.
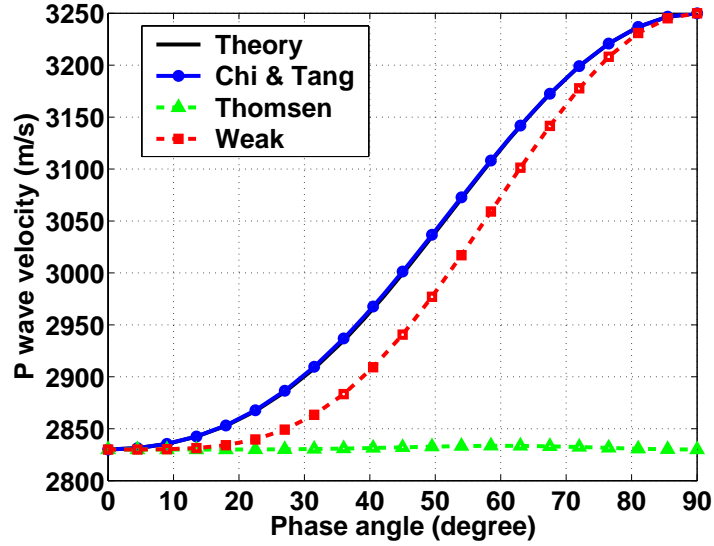
4a

4b

4c

Figure 4: Comparisons of various approximations for (a) qP, (b) qSV, and (c) Stoneley wave velocities.

For *SH* waves, the modulus is expressed in the following form exactly:

$$\mu_{SH} = \rho V_{SH}^2 = c_{44} \cos^2 \theta + c_{66} \sin^2 \theta . \tag{17}$$

Provided that we have cross-dipole and Stoneley logging data in the same well, all the three moduli can be computed, we can solve the linear system of three unknowns, c_{44}, c_{66} and a third complicated term $P = \dfrac{2(\varepsilon - \delta)c_{33}}{1 + 2\varepsilon \sin^2 \theta / f}$. Solving c_{44}, c_{66} and P from equation

(15), (16) and (17) gives the following analytical formulae after complicated manipulation:

$$c_{44} = \left(\mu_{SH} \cos^4 \theta - \mu_{ST} \sin^2 \theta \cos^2 \theta + \frac{1}{8} \mu_{qSV} \sin^4 \theta \right) \Big/ \Delta(\theta), \tag{18}$$

$$c_{66} = \left(\mu_{SH} \left(\frac{1}{8} - \cos^2 \theta \right) \sin^2 \theta + \mu_{ST} \cos^4 \theta - \frac{1}{8} \mu_{qSV} \sin^2 \theta \cos^2 \theta \right) \Big/ \Delta(\theta) \tag{19}$$

$$P = \left[-\mu_{SH} \cos^2 \theta + \mu_{ST} \sin^2 \theta + \mu_{qSV} \left(\cos^2 \theta - \sin^2 \theta \right) \right] \Big/ \left[\Delta(\theta) \sin^2 \theta \right] \tag{20}$$

where
$$\Delta(\theta) = \cos^4 \theta - \sin^2 \theta \cos^2 \theta + \frac{1}{8} \sin^4 \theta . \tag{21}$$

Then the shear anisotropic parameter can be computed simply using the following definition:

$$\gamma = \frac{c_{66} - c_{44}}{2c_{44}}. \tag{22}$$

When equation (21) is equal to zero, the system of equations for inversion becomes singular. Two angles about 47 and 69 degrees satisfy the singular condition (Norris and Sinha, 1993). An optimization algorithm may reduce the inversion errors.

Considering the fact that the measurement of well deviation in the field may not be accurate, we test the sensitivity of the inversion procedures to it. By introducing 1 and 2 degree errors in the well deviation, the inverted parameters are compared with the true value (Zhu et al., 2006). The shear moduli are generally pretty accurate. From Figure 5, for a 1 degree error, the error of γ is small except around 47 degrees, which make the linear system singular. For a 2 degree error, the error of inverted γ is large when well deviations are around 47 and 69 degrees. Therefore, fairly accurate well deviation measurement is desired to accurately obtain γ.
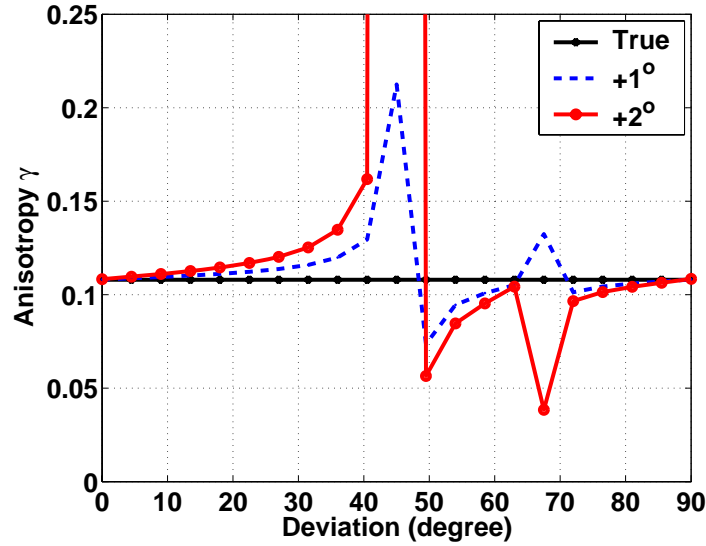
5a
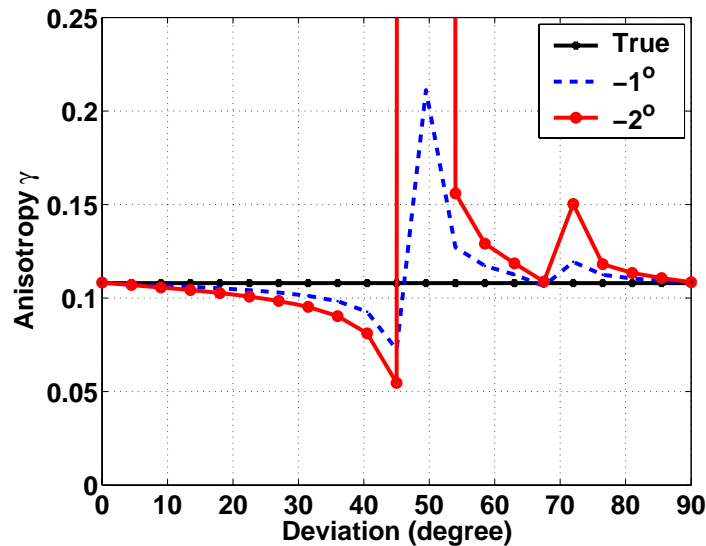
5b

Figure 5: Sensitivity of inverted anisotropy to well deviation errors.

Joint inversion of shear-wave anisotropic parameter using cross-dipole and Stoneley wave anisotropy

Using cross-dipole or Stoneley wave along in deviated wells, formation anisotropy can be assessed to some degree, but the true shear-wave anisotropic parameter cannot be obtained. We try to express the shear anisotropic parameter in terms of Stoneley-wave measured anisotropy and cross-dipole anisotropy and well deviation. This result provides a simple way to obtain the true shear anisotropic parameter using existing anisotropy measurements.

The cross-dipole anisotropy is defined as:

$$\eta = \frac{\mu_{SH} - \mu_{qSV}}{2\mu_{qSV}}.$$

(23)

For convenience, define $N = \frac{2(\varepsilon - \delta)c_{33}/c_{44}}{1 + 2\varepsilon \sin^2 \theta / f}$. Substituting expressions for the moduli, equations (15) and (16), into the definition yields

$$\eta = \frac{\gamma \sin^2 \theta - N \sin^2 \theta \cos^2 \theta / 2}{1 + N \sin^2 \theta \cos^2 \theta}.$$

(24).

The Stoneley-wave measured anisotropy is defined as:

$$\xi = \frac{\mu_{ST} - \mu_{qSV}}{2\mu_{qSV}}$$

(25).

The sum of the two anisotropies can be written as

$$\eta + \xi = \frac{\gamma + N \sin^2 \theta \left(\dfrac{\sin^2 \theta}{16} - \cos^2 \theta \right)}{1 + N \sin^2 \theta \cos^2 \theta}.$$

(26)

Eliminating N from equation (24) and (26) gives a simple expression of γ as

$$\gamma = \frac{\eta \left(\dfrac{\sin^2 \theta}{8} - \cos^2 \theta \right) + \xi \cos^2 \theta}{(1 + 2\eta)\cos^4 \theta - (1 + 2\xi)\sin^2 \theta \cos^2 \theta + \dfrac{\sin^4 \theta}{8}}$$

(27)

We attach the details of the derivation in the appendix.

APPLICATION

We apply our inversion method to laboratory data and field data in this section.

Inversion using Laboratory Data in one borehole

Zhu et al. (2006) used an anisotropic Phenolite as the laboratory material and drilled boreholes at different angles with respect to the slowest P-wave principle axis. From the measured qP, qSV, SH, and Stoneley wave velocities extracted from monopole and dipole logging data, they constructed a equivalent TIV model for the Phenolite to interpret their measurements. Since all the boreholes were drilled in the same symmetry plane, a TI model can fit well for the measured for the qP and qSV wave velocities.
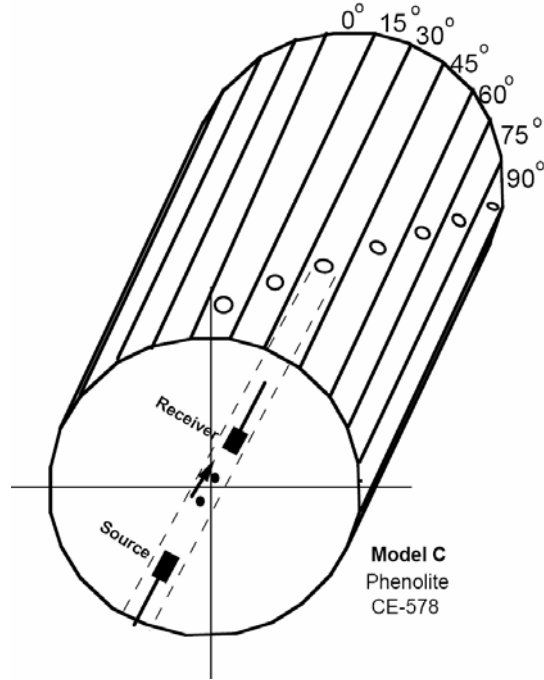
Figure 6. The Phenolite borehole model

We use the same TI model for the laboratory measurements (Table I). We also use the laboratory measured P, SV, and Stoneley wave velocities, and theoretically predicated SH wave velocity for our inversion.

C_{11} (GPa)	c_{33} (GPa)	c_{66} (GPa)	c_{44} (GPa)	c_{12} (GPa)	c_{13} (GPa)
13.94	10.57	3.42	2.97	7.10	5.70

Table 1. The elastic stiffness of an equivalent TI model for the Phenolite block

Shear wave anisotropy is 10.8%. The Stoneley velocity in a horizontal well is only 2.7% higher than the velocity in a vertical well. The measurement errors of Stoneley velocity in wells at 45 to 90 degree deviations are significant comparing to the velocity changes due to well deviation difference. This renders the anisotropy inversion results with relatively large errors. However, except for the results at 45 and 60 degrees, others are still fairly good estimates. Around 45 degrees, the SV wave velocities are not sensitive to the vertical shear wave property as shown in Figure 3b. Therefore, the SV wave velocities around 45 degrees do not have good constraints on inversion results. This is another reason that the inverted anisotropy tends to have large errors.

Angle (degree)	0	15	30	45	60	75	90
Log P	2720	2760	2864	2950	3100	3150	3144
Theory P	2830	2846	2900	2999	3119	3214	3250
Error P (%)	-3.89	-3.00	-1.24	-1.65	-0.61	-1.99	-3.26
Log SV	1452	1463	1516	1554	1493	1489	1433
Theory SV	1460	1488	1539	1556	1526	1481	1460
Error SV (%)	-0.55	-1.70	-1.51	-0.13	-2.15	0.57	-1.85
Theory SH	1460	1471	1499	1537	1574	1600	1610
Log ST	1168	1160	1150	1160	1150	1150	1170
Theory ST	1165	1162	1154	1145	1139	1135	1134
Error ST (%)	0.25	-0.16	-0.35	1.29	1.01	1.34	3.19
Anisotropy (%)	11.5	10.6	8.2	130.4	-4.0	15.5	13.1
Error Anis (%)	6.5	-1.9	-23.8	1107.4	-137.0	43.5	21.3

Table 2. Measured and theoretical velocities of P, SV, and Stoneley waves and the theoretical SH wave velocity used for anisotropic inversion of the TI model. The unit of velocities is m/s. The inverted anisotropy and its errors are shown as well.

Field Example

The new method has been applied to an acoustic logging data set from a deviated well. The well was drilled in Mississippi canyon. The goal is to characterize the TI property of the shale formation from 2800 to 2880 meters. Acoustic cross-dipole and monopole waveform logging data were acquired throughout the formation. The low-frequency end of the monopole data was set to 0.2 kHz to allow for the acquisition of Stoneley waves in the waveform data. Figure 7 shows information about this zone. Track 1 of the figure shows the gamma curve and the deviation curve. The apparent well deviation is about 50 degrees. Track 2 is the migrated scattered fields, from which we can see clearly the dipping of the formation. The dip angle is estimated to be about 33 degrees. The true well deviation with respect the symmetry axis of the TI formation can be obtained as the apparent well deviation less the dip angle. The caliper, density and apparent well deviation logs are also presented in Figure 8.
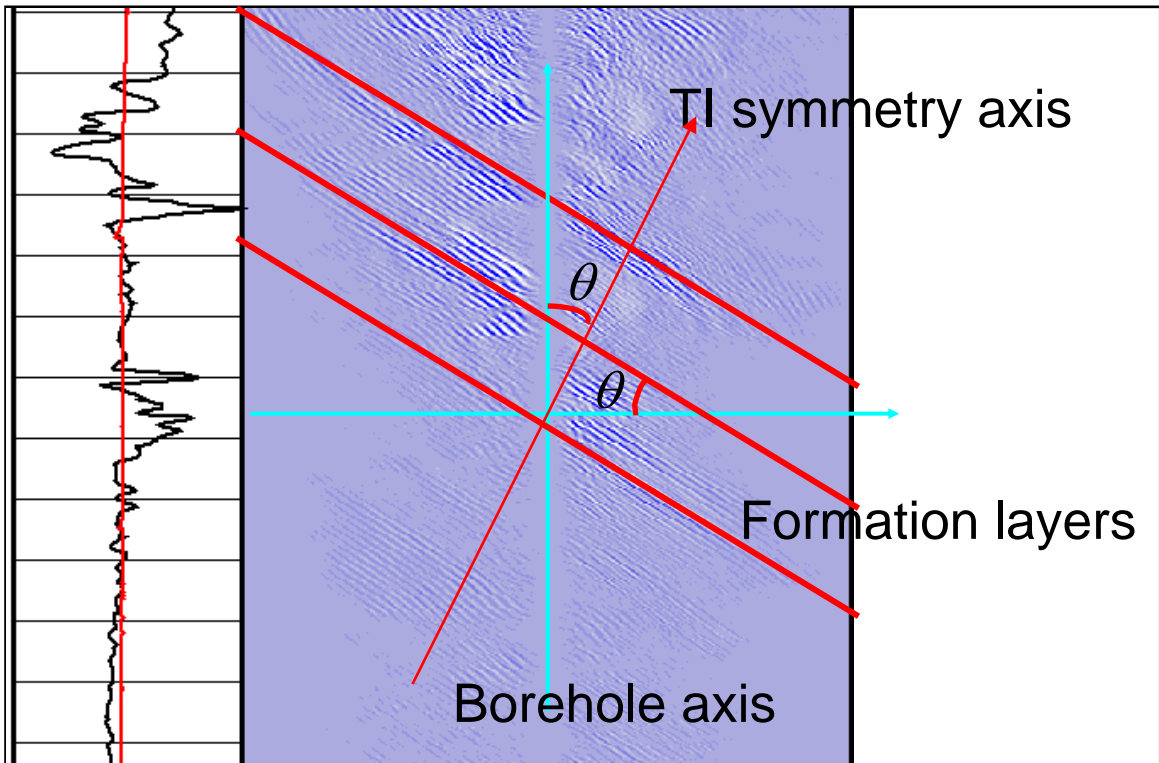
Figure 7: Apparent well deviation and formation image. The red curve in left track is the apparent well deviation, and the right track is the migrated formation image around the wellbore. The center of the right track is the borehole axis.
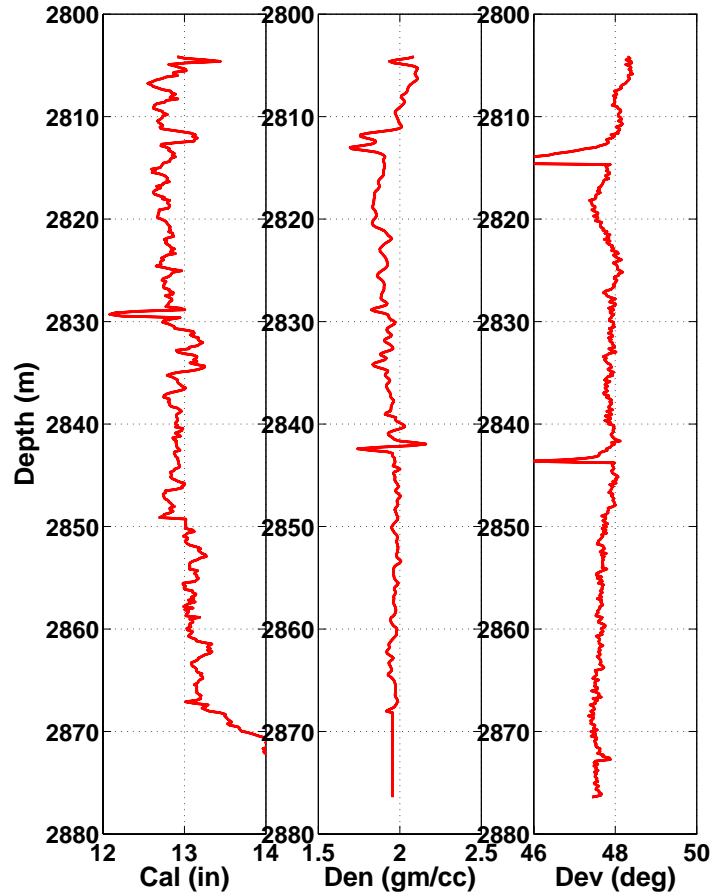
Figure 8: Measured caliper, density and apparent well deviation logs

First, we use the direct inversion method to compute c_{44} and c_{66} (see Figure 9). We see that the inverted c_{66} are consistently higher than c_{44}, which is as expected for realistic shale formations. Then the SH and SV wave velocity logs are computed based on equations (5) and (6).

The computed SH wave velocities are consistently higher than the dipole measurements; the computed SV wave velocities are consistently slower than the dipole measurements (Figure10). This is also consistent with the scenario shown in Figure 1a.
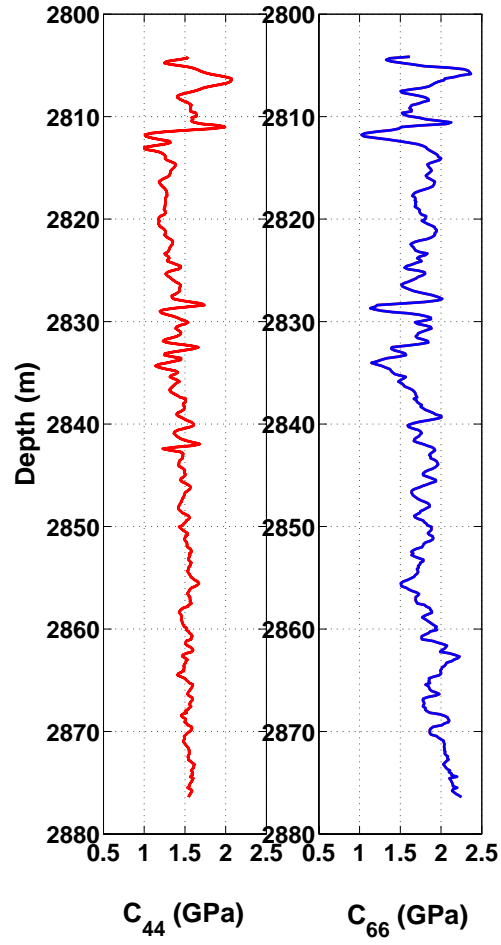
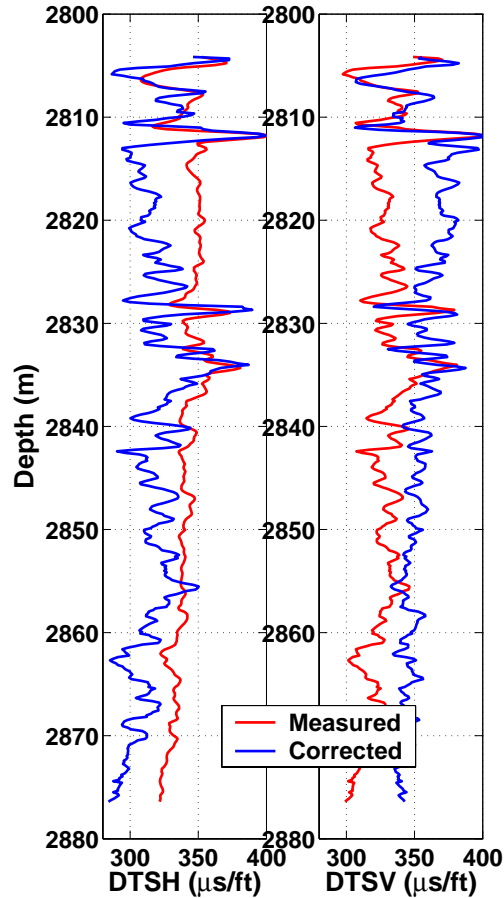**Figure 9: Inverted shear formation modulus logs**

Figure 10: Comparison of measured and corrected vertical and shear wave slowness logs.

Then shear-wave anisotropic parameter γ is calculated. The zero-frequency parameter γ is Stoneley wave modulus is computed using the method developed by Tang (2003). The inverted parameter γ is compared with Stoneley and cross-dipole anisotropic parameters. The cross-dipole anisotropy is generally small in this zone around 10%, while the Stoneley-wave measured anisotropy is around 15%. This is reasonable because the true deviation of this well around 33 degree. The inverted parameter γ is higher than the Stoneley-wave measured anisotropy as expected from theoretical results, and it follows the trend of variation of the Stoneley-wave measured anisotropy curve. However, at the some depth, the inverted parameter γ is lower than the Stoneley-wave measured anisotropy.

Secondly, the cross-dipole and Stoneley-wave measured anisotropy are used with the estimated well deviation to calculate the parameter γ. The inverted parameter γ is slightly different from the previous result. However, they are still in very good agreement. This method is more straightforward.
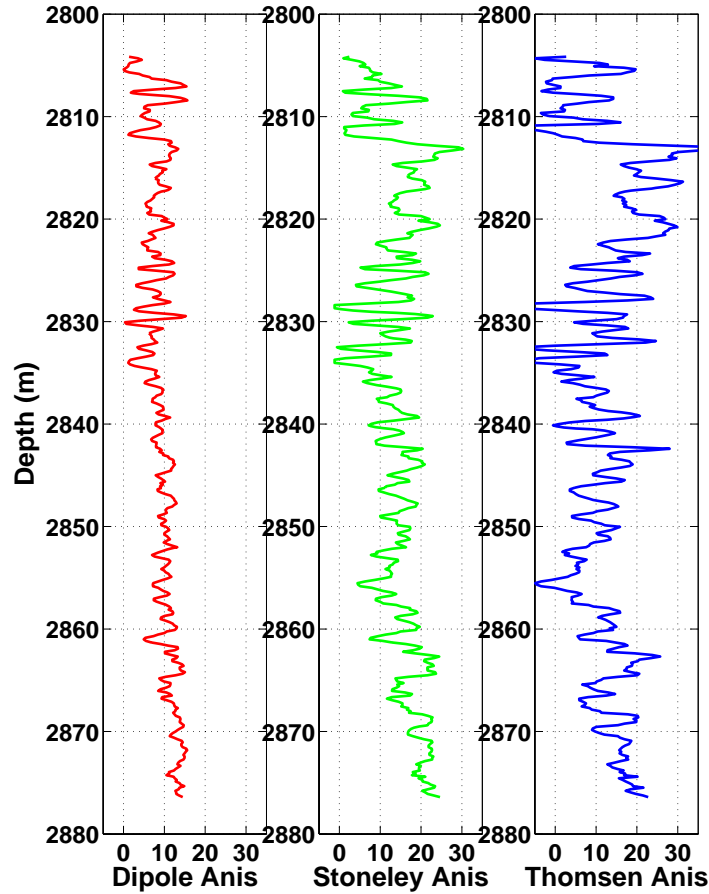
Figure 11: Measured dipole anisotropy, inverted Stoneley anisotropy, and inverted shear wave anisotropy.

Discussion

The proposed TI-estimation method using borehole Stoneley waves has several aspects that need be discussed here. These discussions will help clarify the strength and weakness of the method in practical applications.

Since the Stoneley wave velocity is sensitive to the borehole fluid modulus, we need to understand how the fluid modulus varies as a function of cuttings, temperature and borehole fluid pressure.

As in the shear slowness analysis using Stoneley waves, the Stoneley wave method is applicable mostly in slow formations where the formation shear rigidity is comparable or below the borehole fluid modulus. In this case the Stoneley wave is quite sensitive to formation shear wave properties, isotropic or anisotropic. However, in fast formations, the sensitivity becomes low (Ellefsen, 1990). With the help of the cross-dipole measurements, the shear moduli and shear TI parameter may still be reliably obtained.

Formation permeability will significantly affect the Stoneley wave propagation velocity, especially at low frequencies (Tang et al., 1990). Thus the TI parameter estimation method using low-frequency Stoneley waves is not applicable in permeable formations unless the permeability effect can be accounted for.

The proposed Stoneley-wave estimation method obtains only the shear-wave anisotropy information. However, in seismic migration/imaging using P- and/or converted waves, the P-wave anisotropy parameter ε (Thomsen, 1986) is desired. Fortunately, in many rocks, such as shales, P-wave anisotropy and shear-wave anisotropy are strongly correlated (Thomsen, 1986; Wang, 2001). In this case, the shear-wave anisotropy can be correlated with the P-wave anisotropy data to delineate the magnitude and variation of the latter anisotropy. In this regard, the obtained shear-wave anisotropy still provides important information for seismic migration/imaging. Even better, we can possibly utilize the P wave measurement and the correlation in additional to our inverted shear moduli, to obtain all the 5 elastic constants of a TI formation. The anisotropy parameters ε and δ can then be calculated easily.

The earth formations are not horizontal in general. Therefore, we must be able to find out formation dip through scattered wave migration or some other methods. The well deviation must be fairly accurately given to obtain the true anisotropic parameters. If the well deviation is around 47 and 69 degrees, the inversion must be done carefully.

In deviated wells, cross-dipole measurement usually consists of fast and slow waves, corresponding to SH and qSV waves. In most cases, qSV wave is slower than SH wave. However, in some formations, qSV wave can become the fast wave in cross-dipole measurement (Figure 1a). Therefore, we may need the polarization information to decide which one of the two measurements corresponds to the qSV wave. Then the computed qSV and SH moduli can be used to invert for parameter γ.

CONCLUSIONS

We create a linear inversion scheme to estimate shear wave anisotropy using SH, SV, and Stoneley wave velocities logged in one well. Using sensitivity analysis, we find Stoneley wave velocity has good sensitivity to qSV and SH wave velocities in deviated wells. The approximations to qSV and Stoneley wave velocities for strongly anisotropic formations make the linear inversion possible.
Application of the method to laboratory data from boreholes with deviations of 0, 15, 30, 75 and 90 degrees yields fairly good estimation of the shear wave anisotropy of the Phenolite material. For boreholes at 45 and 60 degrees, due to the near-singularity of the system of equations for linear inversion, the inverted anisotropies show significant difference from the know value.
Application of the method to a field data set acquired in a well with about 33 degree true deviation yields a continuous profile of the shale formation. The inverted shear wave anisotropy log shows higher anisotropy variation with depth than the apparent anisotropy measured by cross-dipole data and the anisotropy inverted by Tang's method for vertical wells. The inverted SH wave velocities are consistently higher than the dipole

measurements; the inverted SV wave velocities are consistently slower than the dipole measurements.

ACKNOWLEDGEMENTS

REFERENCES

Chi, S., and X. M. Tang, 2003, Accurate approximations to *qSV* and *qP* wave velocitys in TIV media and Stoneley-wave velocity in general anisotropic media: 44th Society of Professional Well Log Analysts Logging Symposium, Paper OO.

Ellefsen, K. J, 1990, Elastic wave propagation along a borehole in an anisotropic medium, Sc.D. Thesis, Massachusetts Institute of Technology, Cambridge, Massachusetts, USA.

Ellefsen, K. J., M. N. Toksoz, K. M. Tubman, and C. H. Cheng, 1992, Estimating a shear modulus of a transversely isotropic formation: Geophysics, 57, 1428-1434.

Li, X.-Y., H. Dai, M. C. Mueller, O. I. Barkved, 2001, Compensating for the effects of gas clouds on C-wave imaging: A case study from Valhall: The Leading Edge, 20, 1022-1028.

Norris, A. N., 1990, The velocity of a tube wave: Journal of the Acoustical Society of America, 87, 414-417.

Norris, A. N., and B. K. Sinha, 1993, Weak elastic anisotropy and the tube wave: Geophysics, 58, 1091-1098.

Ren, J., C. Gerrard, J. Mcclean, and M. Orlovich, 2005, Prestack wave-equation depth migration in VTI media: The Leading Edge, 24, 618-620.

Rice, J. A., 1987, A method for logging shear wave velocity anisotropy: 57th Annual International Meeting, SEG, Expanded Abstract, 27-28.

Tang, X. M., Cheng, C. H., and Toksoz, M. N., 1991, Dynamic permeability and borehole Stoneley waves: A simplified Biot-Rosenbaum model: Journal of Acoustical Society of America, 90, 1632-1646.

Tang, X. M., 2003, Determining formation shear wave transverse isotropy from borehole Stoneley-wave measurements: Geophysics, 68, 118-126.

Thomsen, L., 1986, Weak elastic anisotropy: Geophysics, 51, 1954-1966.

Tsvankin, I., 1995, Body-wave radiation patterns and AVO in transversely isotropic media: Geophysics, 60, 1409-1425.

Wang, Z., 2001, Seismic anisotropy in sedimentary rocks, part 2: Laboratory data: Geophysics, 67, 1423-1440.

Zhu, X., S. Altan, and J. Li, 1999, Recent advances in multicomponent processing: The Leading Edge, 18, 1283-1288.

Zhu, Z., S. Chi, M. N. Toksöz, 2006, Sonic Logging in Deviated Boreholes of an Anisotropic Formation: Laboratory Study, MIT Earth Resouces Laboratory Industrial Consortia Report.

Appendix: Derivation of the joint inversion formula of shear-wave anisotropic parameter using cross-dipole and Stoneley wave anisotropy

Let's list again the formulae of the moduli of *SH, qSV* and Stoneley waves:

$$\mu_{SH} = \rho V_{SH}^2 = c_{44} \cos^2 \theta + c_{66} \sin^2 \theta , \qquad (A1)$$

$$\mu_{qSV} = \rho V_{qSV}^2 = c_{44} + \frac{2(\varepsilon - \delta)c_{33}\sin^2\theta\cos^2\theta}{1 + 2\varepsilon\sin^2\theta/f}, \tag{A2}$$

$$\mu_{ST} = c_{44}\sin^2\theta + c_{66}\cos^2\theta + \frac{1}{4}\frac{(\varepsilon - \delta)c_{33}\sin^4\theta}{1 + 2\varepsilon\sin^2\theta/f}, \tag{A3}$$

where ε and δ are anisotropic parameters (Thomsen, 1986) and $f = 1 - \dfrac{c_{44}}{c_{33}}$.

Then let's re-introduce three definitions of anisotropy.

The cross-dipole anisotropy is defined as:

$$\eta = \frac{\mu_{SH} - \mu_{qSV}}{2\mu_{qSV}}, \tag{A4}$$

The Stoneley-wave measured anisotropy is defined as:

$$\xi = \frac{\mu_{ST} - \mu_{qSV}}{2\mu_{qSV}}, \tag{A5}$$

The shear-wave TI anisotropy is defined as:

$$\gamma = \frac{c_{66} - c_{44}}{2c_{44}}, \tag{A6}$$

For convenience, define $N = \dfrac{2(\varepsilon - \delta)c_{33}/c_{44}}{1 + 2\varepsilon\sin^2\theta/f}$. Substituting equation (A1), (A2) and (A6) into (A4) yields:

$$
\begin{aligned}
\eta &= \frac{(c_{66} - c_{44})\sin^2\theta - Nc_{44}\sin^2\theta\cos^2\theta}{2c_{44} + 2Nc_{44}\sin^2\theta\cos^2\theta} \\
&= \frac{2c_{44}\gamma\sin^2\theta - Nc_{44}\sin^2\theta\cos^2\theta}{2c_{44} + 2Nc_{44}\sin^2\theta\cos^2\theta} \\
&= \frac{\gamma\sin^2\theta - N\sin^2\theta\cos^2\theta/2}{1 + N\sin^2\theta\cos^2\theta}
\end{aligned}
\tag{A7}
$$

Solving N from equation (A7) yields:

$$N = \frac{\gamma\sin^2\theta - \eta}{(1/2 + \eta)/\sin^2\theta\cos^2\theta} \tag{A8}$$

The sum of the Stoneley and cross-dipole anisotropy can be written as:

$$\eta + \xi = \frac{\mu_{SH} + \mu_{ST} - 2\mu_{qSV}}{2\mu_{qSV}}$$

$$= \frac{c_{66} - c_{44} + 2Nc_{44}\sin^2\theta\left(\dfrac{\sin^2\theta}{16} - \cos^2\theta\right)}{2c_{44} + 2Nc_{44}\sin^2\theta\cos^2\theta} \tag{A9}$$

$$= \frac{\gamma + N\sin^2\theta\left(\dfrac{\sin^2\theta}{16} - \cos^2\theta\right)}{1 + N\sin^2\theta\cos^2\theta}$$

Expanding equation (A9) gives:

$$\eta + \xi + (\eta + \xi)N\sin^2\theta\cos^2\theta = \gamma + N\sin^2\theta\left(\frac{\sin^2\theta}{16} - \cos^2\theta\right) \tag{A10}$$

$$\gamma = \eta + \xi + (1 + \eta + \xi)N\sin^2\theta\cos^2\theta - N\frac{\sin^2\theta}{16\cos^2\theta} \tag{A11}$$

Plugging N into equation (A11) yields:

$$\gamma = \eta + \xi + (1 + \eta + \xi)\frac{\gamma\sin^2\theta - \eta}{1/2 + \eta} - \frac{(\gamma\sin^2\theta - \eta)\sin^2\theta}{16\cos^2\theta(1/2 + \eta)} \tag{A12}$$

Gathering terms of γ gives:

$$\gamma\left(1 - (1 + \eta + \xi)\frac{\sin^2\theta}{1/2 + \eta} + \frac{\sin^4\theta}{16\cos^2\theta(1/2 + \eta)}\right)$$

$$= \eta + \xi - \frac{\eta(1 + \eta + \xi)}{1/2 + \eta} + \frac{\eta\sin^2\theta}{16\cos^2\theta(1/2 + \eta)} \tag{A13}$$

Multiplying both sides of equation (A13) by $2(1/2 + \eta)\cos^2\theta$ gives:

$$\gamma\left((2\eta + 1)\cos^2\theta - 2(1 + \eta + \xi)\sin^2\theta\cos^2\theta + \frac{\sin^4\theta}{8}\right)$$

$$= (2\eta + 1)(\eta + \xi)\cos^2\theta - 2\eta(1 + \eta + \xi)\cos^2\theta + \frac{\sin^2\theta}{8}\eta \tag{A14}$$

Simplifying equation (A14) yields:

$$\gamma\left(2\eta\cos^2\theta - 2\eta\sin^2\theta\cos^2\theta - 2\xi\sin^2\theta\cos^2\theta + \cos^2\theta - 2\sin^2\theta\cos^2\theta + \frac{\sin^4\theta}{8}\right)$$

$$= (\eta + \xi)\cos^2\theta - 2\eta\cos^2\theta + \frac{\sin^2\theta}{8}\eta \tag{A15}$$

Applying trigonometric relationships yields:

$$\gamma\left(2\eta\cos^4\theta - 2\xi\sin^2\theta\cos^2\theta + \cos^4\theta - \sin^2\theta\cos^2\theta + \frac{\sin^4\theta}{8}\right)$$

$$= (\eta+\xi)\cos^2\theta - 2\eta\cos^2\theta + \frac{\sin^2\theta}{8}\eta$$

(A16)

After minimum algebraic manipulation, one gets the simple expression of γ as follows:

$$\gamma = \frac{\eta\left(\dfrac{\sin^2\theta}{8} - \cos^2\theta\right) + \xi\cos^2\theta}{(1+2\eta)\cos^4\theta - (1+2\xi)\sin^2\theta\cos^2\theta + \dfrac{\sin^4\theta}{8}}$$

(A17)

In two special cases, when $\theta = \dfrac{\pi}{2}$, $\gamma = \eta$, the cross-dipole anisotropy; when $\theta = 0$, $\eta = 0$, and $\gamma = \dfrac{\xi-\eta}{1+2\eta} = \xi$, the Stoneley-wave measured anisotropy.